IOSR Journal of Mechanical and Civil Engineering (IOSR-JMCE)
e-ISSN: 2278-1684,p-ISSN: 2320-334X, Volume 18, Issue 2 Ser. III (Mar. – Apr. 2021), PP 25-37
www.iosrjournals.org

MHD Free Convection Heat and Mass Transfer on a Vertical Plate Embedded in Porous Medium

M. Jahir[1], A. Saha[2*], M. Ali[2]
[1]*Department of Mathematics, Feni Government College, Feni-3900, Bangladesh*
[2]*Simulation Lab, Department of Mathematics, Chittagong University of Engineering & Technology, Chattogram-4349, Bangladesh*
Corresponding Author: M. Jahir

Abstract
Natural convection heat and mass transfer flow have been studied in presence of magnetic field on a vertical plate embedded in porous media. The governing equations make dimensionless using usual transformation. The numerical solution has obtained employing explicit finite difference method. The influence of entering physical parameters on the velocity, temperature and concentration profiles as well as local and average shear stress, Sherwood number and Nusselt number have discussed and presented graphically.

Keyword*: Free convection, Porous Medium, Explicit Finite Difference, Magneto hydrodynamics, Heat and Mass Transfer*

Date of Submission: 10-04-2021 Date of Acceptance: 26-04-2021

I. Introduction

Magneto hydrodynamics (MHD) is the branch of physics which study the magnetic properties and behavior of electrically conducting fluids. Hannes Alfvens [1] at first was initiated the field of MHD for which he received the Novel prize in physics in 1970. MHD has a wide range of application such as Geophysics, Earthquakes, Astrophysics, Sensors, Engineering (such as plasma confinement, liquid-metal cooling of nuclear reactors and electromagnetic casting), and biomedical engineering (like Magnetic drug targeting, magnetic devices for cell separation, cancer tumour treatment, magnetic endoscopy, and cell death by hyperthermia which is created by an alternating magnetic field [2] are the example of few. Due to its importance MHD has attracted a great deal of interest to the physics community.

A solid body or material which contains pores (small void space) [3] is known as porous media. The pores are usually filled with a fluid such as liquid or gas. The pores are distributed less or more frequently throughout the material. In connection with much geological application (such as soil mechanics, ground water hydrology and petroleum engineering) the study of flow through porous media is important. Depending on the size, arrangement and shape of the pores, as well as the porosity (the ratio of the total pore volume relative to the apparent volume of the material) and composition of the material itself the characteristics of a porous material are varied. The conception of porous media is used in many areas of applied science and engineering such as filtration mechanics, Engineering, Geoscience, Biology and Biophysics, and Material Science etc. Convection in porous media has application in geothermal energy recovery, oil extraction, thermal energy storage and flow through filtering devices. Because of various applications the problems of MHD flow with heat and mass transfer flow in a porous medium has attracted the attention of researchers. The free convection flow arises frequently in nature, flows of fluid through porous media in presence of magnetic field are of main interest and have attracted by many researchers due to their applications in the science and technology**.**

El-Arabawy [4] has investigated the effects of Prandtl number, the radiation parameter, and porosity parameter on the flow of micropolar fluid for a continuous moving plate in presence of radiation and they found that the heat transfer rate is increasing for the effects of suction, radiation parameter, and Prandlt number, on the other hand that of decreasing for injection.

Natural convection heat and mass transfer in porous medium have studied Bejan and Khair [5]. In a channel filled with porous medium the exact solution of an oscillatory MHD flow has investigated by Singh [6]. Raghunath et al. [7] have studied MHD heat and mass transfer flow considering incompressible electrically conducting fluid in presence of transverse magnetic field. The medium is porous enclose between two vertical porous plates. The solutions for velocity, temperature and concentration profiles have determined by regular perturbation technique. Influences of concerned physical parameters on velocity, temperature and concentration have discussed. In presence of radiation and chemical reaction the visco-elastic natural convection heat and mass transfer flow through porous medium have studied by Choudhury and Das [8]. They have solved the

governing equations for velocity, temperature and concentration equations employing multiple perturbation technique and the influence of entering parameters on velocity, temperature and concentration profiles have shown graphically. Reddy and Sreedevi [9] have investigated the boundary layer heat and mass transfer flow through porous medium for nanofluid in presence of magnetic field with chemical reaction and thermal radiation over an inclined plate. Keya [10] have studied the effect of conjugate heat transfer on steady mixed convection heat transfer flow over a thin vertical plate embedded in a porous medium with high porosity in presence of magnetic field. Being motivated in this manuscript the free convection heat and mass transfer flow has studied on a vertical plate embedded in porous medium. The manuscript is arranged as: In sequence of introduction governing equations present in **section 2**. Mathematical formation and numerical solution provide in **section3**. In **section 4** incorporates the expression of shear stress, Nusselt and Sherwood numbers. The results and discussion are presented in **section 5.** Finally the important results summarize in **section 6.**

II. Model Equations

The unsteady free convection flow of a viscous incompressible fluid about a vertical plate with heat and mass transfer in presence magnetic field embedded in porous medium have investigated. The flow is assumed to be in x-direction and magnetic field is normal to it.

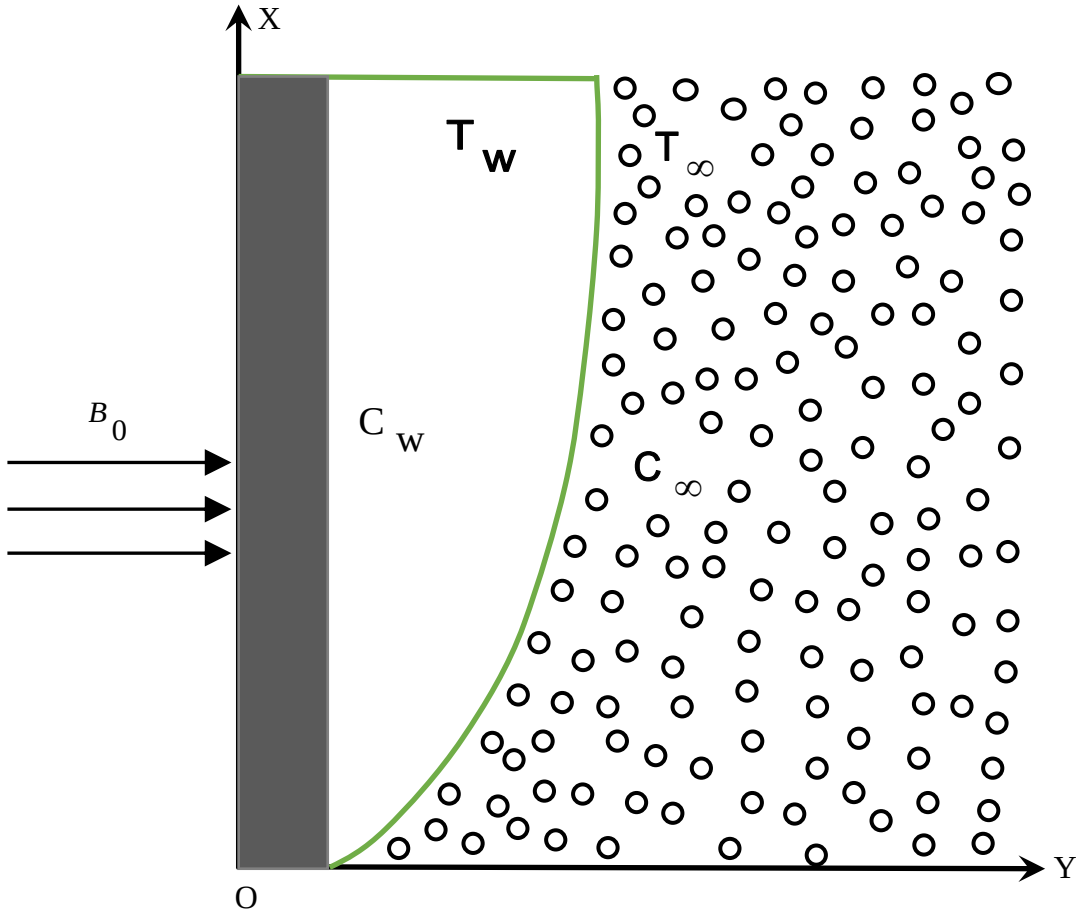

Figure 1: Physical configuration and coordinates

Let us assumed, unsteady MHD flow of an incompressible viscous fluid along the vertical plate. Instantaneously at time $t > 0$ temperature of the plate and species concentration are raised to ($T_w (> T_\infty)$ and $C_w (> C_\infty)$ respectively, which are there after maintained constant, where T_w, C_w are temperature and concentration at the wall and T_∞, C_∞ are temperature and concentration outside the boundary layer, respectively. A uniform magnetic field $\mathbf{B} = (0, B_o, 0)$ has considered normal to the plate and induced magnetic field is supposed to be negligible. B_0 is the constant magnetic field strength. Using relation $\nabla . \mathbf{J} = 0$ for

current density $J = (J_x, J_y, J_z)$ one can be obtained $J_y =$ constant. Since the plate is assumed to be non-conducting, therefore $J_y = 0$ at the plate and hence zero everywhere. The generalized Ohm's law in the absence of electric field for weakly ionized fluid is of the form $\mathbf{J} = \sigma(\mathbf{E} + \mathbf{q} \times \mathbf{B})$ .Since no polarized voltage exists, so the polarization effect of the fluid is negligible i.e. $\mathbf{E} = (0, 0, 0)$

Therefore from Ohm's law J_x can be determined as $J_x = \frac{1}{\rho} B_0^2$. The physical configuration of the problems has been shown in Fig.1. Under the above assumptions and employing Boussinesq approximation continuity, momentum, energy, and concentration equations one can obtain as

continuity equation

$$\frac{\partial u}{\partial x} + \frac{\partial v}{\partial y} = 0 \ , \tag{1}$$

momentum equation

$$\frac{\partial u}{\partial t} + u\frac{\partial u}{\partial x} + v\frac{\partial u}{\partial y} = \nu\frac{\partial^2 u}{\partial y^2} + g\beta(T - T_\infty) + g\beta^*(C - C_\infty) - \frac{\sigma B_0^2}{\rho}u - \frac{\nu}{\kappa}u \ , \tag{2}$$

energy equation

$$\frac{\partial T}{\partial t} + u\frac{\partial T}{\partial x} + v\frac{\partial T}{\partial y} = \frac{\kappa}{\rho C_p}.\frac{\partial^2 T}{\partial y^2} + \frac{\nu}{C_p}\left(\frac{\partial u}{\partial y}\right)^2 \ , \tag{3}$$

and concentration equation

$$\frac{\partial C}{\partial t} + u\frac{\partial C}{\partial x} + v\frac{\partial C}{\partial y} = D_m.\frac{\partial^2 C}{\partial y^2} \ , \tag{4}$$

with boundary conditions

$u = U_0, v = 0, T = T_w, C = C_w \quad at \quad y = 0$

$u \to 0, T \to T_\infty, C \to C_\infty \quad as \quad y \to \infty$

where ν is the kinematic viscosity, g is the acceleration due to gravity, ρ is the fluid density, β is the coefficient of volumetric expansion, β^* is the co-efficient of expansion with concentration, σ is the electric conductivity, T is the temperature of the fluid inside the thermal boundary layer, T_∞ is the temperature in the free stream, C is the concentration in the boundary layer, C_∞ is the concentration outside the boundary layer, C_p is the specific heat with constant pressure, κ is the thermal conductivity, D_m is the co-efficient of mass diffusivity, and U_0 is the constant indicates the uniform velocity of the fluid.

III. Mathematical Formulation and Numerical Solution

Using the usual transformations

$$u = U_0 U, v = V U_0, Y = \frac{yU_0}{\nu}, X = \frac{xU_0}{\nu}, \eta = \frac{tU_0^2}{\nu}$$

$T = T_\infty + (T_w - T_\infty)\overline{T}, C = C_\infty + (C_w - C_\infty)\overline{C}$ into the Eqs. (1), (2), (3) and (4) after some mathematical manipulation one can obtain the following dimensionless non-linear ordinary differential equations as

continuity equation

$$\frac{\partial U}{\partial X} + \frac{\partial V}{\partial Y} = 0 \ , \tag{5}$$

momentum equation

$$\frac{\partial U}{\partial \eta} + U\frac{\partial U}{\partial X} + V\frac{\partial U}{\partial Y} = \frac{\partial^2 U}{\partial Y^2} + Gr\,\overline{T} + Gm\,\overline{C} - MU - NU \ , \tag{6}$$

energy equation

$$\frac{\partial \overline{T}}{\partial \eta} + U\frac{\partial \overline{T}}{\partial X} + V\frac{\partial \overline{T}}{\partial Y} = \frac{1}{Pr}\frac{\partial^2 \overline{T}}{\partial Y^2} + Ec\left(\frac{\partial U}{\partial Y}\right)^2, \tag{7}$$

and concentration equation

$$\frac{\partial \overline{C}}{\partial \eta} + U\frac{\partial \overline{C}}{\partial X} + V\frac{\partial \overline{C}}{\partial Y} = \frac{1}{Sc}\frac{\partial^2 \overline{C}}{\partial Y^2} \tag{8}$$

with boundary conditions

$U = 1, V = 0, \overline{T} = 1, \overline{C} = 1 \text{ at } Y = 0$

$U = 0, \overline{T} = 0, \overline{C} = 0 \text{ as } Y \to \infty$

Where Grashof number, $Gr = \frac{\nu g\beta(T_w - T_\infty)}{U_0^3}$, modified Grashof number, $Gm = \frac{\nu g\beta^*(C_w - C_\infty)}{U_0^3}$, magnetic parameter, $M = \frac{\sigma \nu B_0^2}{\rho U_0^2}$, porosity parameter, $N = \frac{\nu^2}{\kappa U_0^2}$, Prandtl number, $Pr = \frac{\nu}{\alpha}$, Eckert number, $Ec = \frac{U_0^2}{C_p(T_w - T_\infty)}$, Schmidt number, $Sc = \frac{\nu}{D_m}$.

The non-dimensional set of nonlinear ordinary differential equations one can be solved numerically with boundary conditions along with explicit finite difference method.

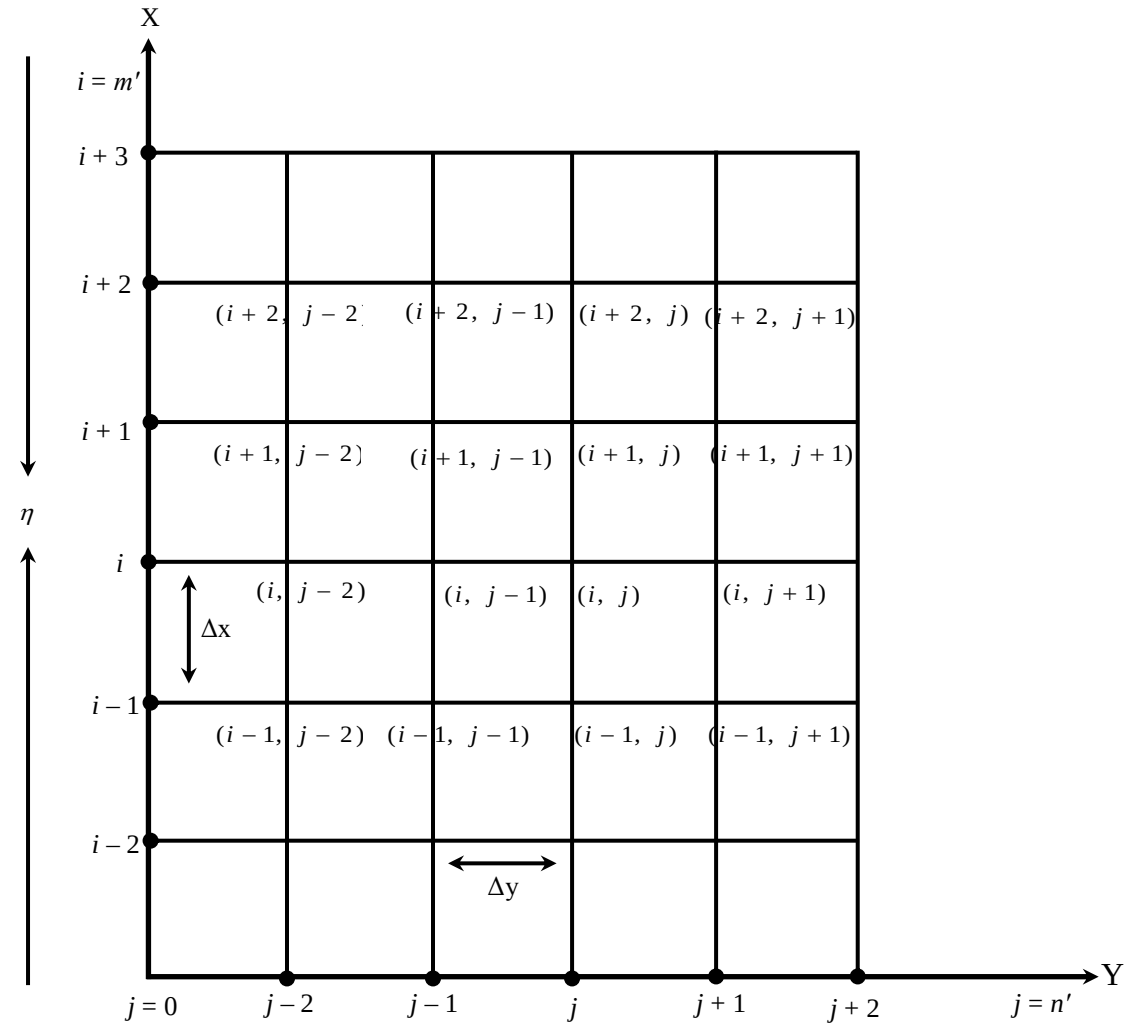

Figure 2: Explicit finite difference grid spacing

To obtain the difference equations the region of the flow is divided into a grid or mesh of lines parallel to X - and Y -axes, where X - axis is taken along flow of the fluid and Y - axis is normal to the flow of the fluid. In this study the height of plate $X_{\max}$ (=100) has considered, that is, X varies from 0 to 100 and $Y_{\max}$ =25 as corresponding to $Y \to \infty$, that is, Y varies from 0 to 25. There are $m' = 250$ and $n' = 250$ grid spacing in the X - and Y -directions, respectively. Taking $\Delta x = 0.4(0 \le x \le 100)$ and $\Delta Y = 0.1(0 \le Y \le 25)$ with the smaller time step $\Delta \eta = 0.005$. U', $\overline{T'}$ and $\overline{C'}$ have considered for U , $\overline{T}$ and $\overline{C}$ at the end of time- step, respectively.

With help of the explicit finite difference method Eqs.(5)- (8) can be expressed as:

$$\frac{U_{i,j} - U_{i,j-1}}{\Delta X} + \frac{V_{i,j} - V_{i,j-1}}{\Delta Y} = 0 \tag{9}$$

$$U'_{i,j} = U_{i,j} + \Delta\eta \left(\begin{array}{l} -U_{i,j} \dfrac{U_{i,j} - U_{i-1,j}}{\Delta X} - V_{i,j} \dfrac{U_{i,j+1} - U_{i,j}}{\Delta Y} \\ + \dfrac{U_{i,j+1} - 2U_{i,j} + U_{i,j-1}}{(\Delta Y)^2} + \mathrm{Gr}\,\overline{T}_{i,j} + \mathrm{Gm}\,\overline{C}_{i,j} - MU_{i,j} - NU_{i,j} \end{array} \right)$$

(10)

$$\overline{T}'_{i,j} = \overline{T}_{i,j} + \Delta\eta \left(-U_{I,J} \frac{\overline{T}_{i,j} - \overline{T}_{i-1,j}}{\Delta X} - V_{i,j} \frac{\overline{T}_{i,j+1} - \overline{T}_{i,j}}{\Delta Y} + \frac{1}{\mathrm{Pr}} \frac{\overline{T}_{i,j+1} - 2\overline{T}_{i,j} + \overline{T}_{i,j-1}}{(\Delta Y)^2} + \mathrm{Ec} \left(\frac{U_{i,j+1} - U_{i,j}}{\Delta Y} \right)^2 \right)$$

(11)

$$\overline{C}'_{i,j} = \overline{C}_{i,j} + \Delta\eta \left(-U_{i,j} \frac{\overline{C}_{i,j} - \overline{C}_{i-1,j}}{\Delta X} - V_{i,j} \frac{\overline{C}_{i,j+1} - \overline{C}_{i,j}}{\Delta Y} + \frac{1}{Sc} \frac{\overline{C}_{i,j+1} - \overline{C}_{i,j} + \overline{C}_{i,j-1}}{(\Delta Y)^2} \right) \tag{12}$$

with boundary conditions

$U^n_{i,0} = 1,\ V^n_{i,0} = 0,\ \overline{T}^n_{i,0} = 1\ \overline{C}^n_{i,0} = 1$

$U^n_{i,L} = 0,\ \overline{T}^n_{i,L} = 0,\ \overline{C}^n_{i,L} = 0$, where $L \to \infty$.

Here, i and j indicate the grid points along X - and Y - axes, respectively, $\overline{T}$ is the temperature and $\overline{C}$ is the concentration. The convergence criteria in this study are $\mathrm{Pr} \ge 1$ and $Sc \ge 0.22$.

IV. Shear Stress, Nusselt and Sherwood Numbers

The shear stress, Nusselt number and Sherwood number are the quantities of chief physical interests. The Local shear stress and average shear stress in x-direction are defined by $\tau_{xL} = \mu_0 \left(\frac{\partial u}{\partial y} \right)_{y=0}$ and $\tau_{xA} = \mu_0 \left(\frac{\partial u}{\partial y} \right) dx$, which are proportional to $\left(\frac{\partial U}{\partial y} \right)_{Y=0}$ and $\int_0^{100} \left(\frac{\partial U}{\partial Y} \right) dX$, respectively. One the other hand, the local Nusselt number and average Nusselt number are presented by the relation $N_{uL} = -\mu_0 \left(\frac{\partial T}{\partial y} \right)_{y=0}$, $N_{xA} = -\mu_0 \frac{\partial T}{\partial y} dx$, respectively which are proportional to $\left(\frac{\partial \overline{T}}{\partial Y} \right)_{y=0}$ and

$\int_0^{100} \frac{\partial \overline{T}}{\partial Y} dX$, while the local and average Sherwood number are defined by $S_{hL} = -\mu_0 \left(\frac{\partial C}{\partial y} \right)_{y=0}$ and $S_{hA} = -\mu_0 \int \frac{\partial C}{\partial y} dx$ which are proportion to $\left(\frac{\partial \overline{C}}{\partial Y} \right)_{y=0}$ and $\int_0^{100} \frac{\partial \overline{C}}{\partial Y} dX$, respectively.

V. Results and Discussion

To observe the physical circumstances of the problem the velocity, temperature and concentration profiles as well as the shear stress, Nusselt number and Sherwood number have presented graphically.

Figure 3(a) illustrates the effect of magnetic parameter (M) on velocity profile (U). It is seen from this figure that the velocity profile is decreasing for increasing values of M which is expected. The effect of M on local and average shear stress elucidates in Fig. 3(b) and Fig. 3(c) and it is shown that both local and average shear stress is decreasing. It is fact that, due to presence of a transverse magnetic field to the electrically conducting fluid gives to rise a body force like Lorentz force which tends to resist the fluid flow and slowdown its motion in the boundary layer region of the fluid, as a result the velocity profile, local shear stress and average shear stress decrease.

Figure 4 (a) demonstrates the effect of M on temperature profile and it is observed that the temperature of the fluid increases in $0 \leq Y \leq 1.2$ (approx .) and then decreased for the increasing values of M .The local and average Sherwood numbers also decrease for increasing values of M depict Fig. 4(b) and 4(c), respectively. The effect of Gr on velocity profile, local shear stress and average shear stress depict in Figs. 5(a), 5(b) and 5(c), respectively. It is seen from Fig. 5(a) that the velocity profile increased for increasing values of Gr which leads to raise the velocity due to the thermal buoyancy force which induces pressure gradient. This implies that the thermal buoyancy force accelerates the velocity. The fluid velocity attains a maximum value near the plate and then decays to the free stream value. Figures 5(b) and 5(c) illustrate that both local shear stress and average shear stress are increasing due to enhancement of Gr . It is fact that, increase in the values of Gr has the tendency to increase the thermal buoyancy effect. This gives rise to an increase in the induced flow. As a result both local shear stress and average shear stress are increased.

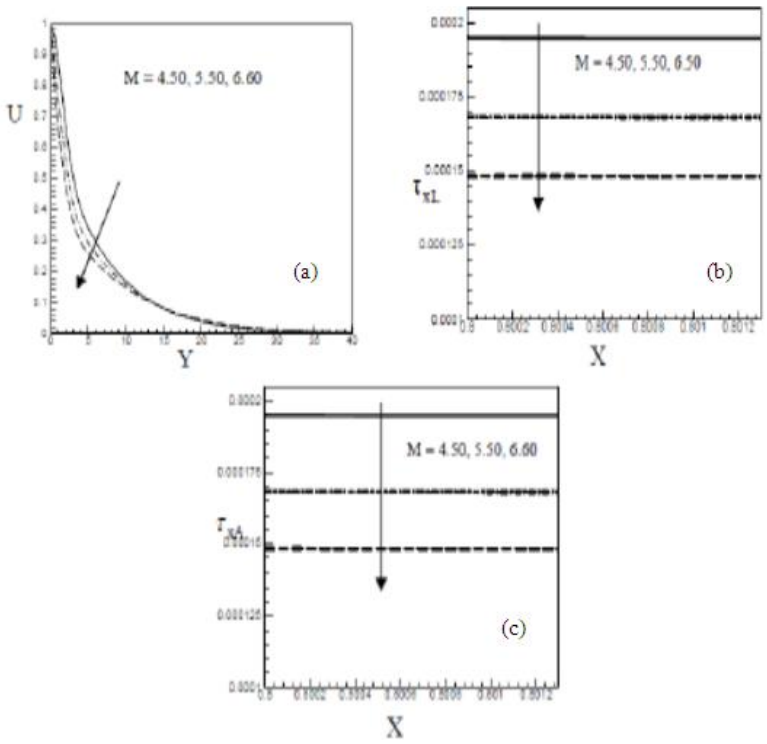

Figure 3 Effect of magnetic parameter (M) on (a) velocity profile, (b) local shear stress and (c) average shear stress taking Gr =2.50,Gm = 2.50, Pr = 7.00, Ec = 0.01, Sc = 0.22, and N = 0.01

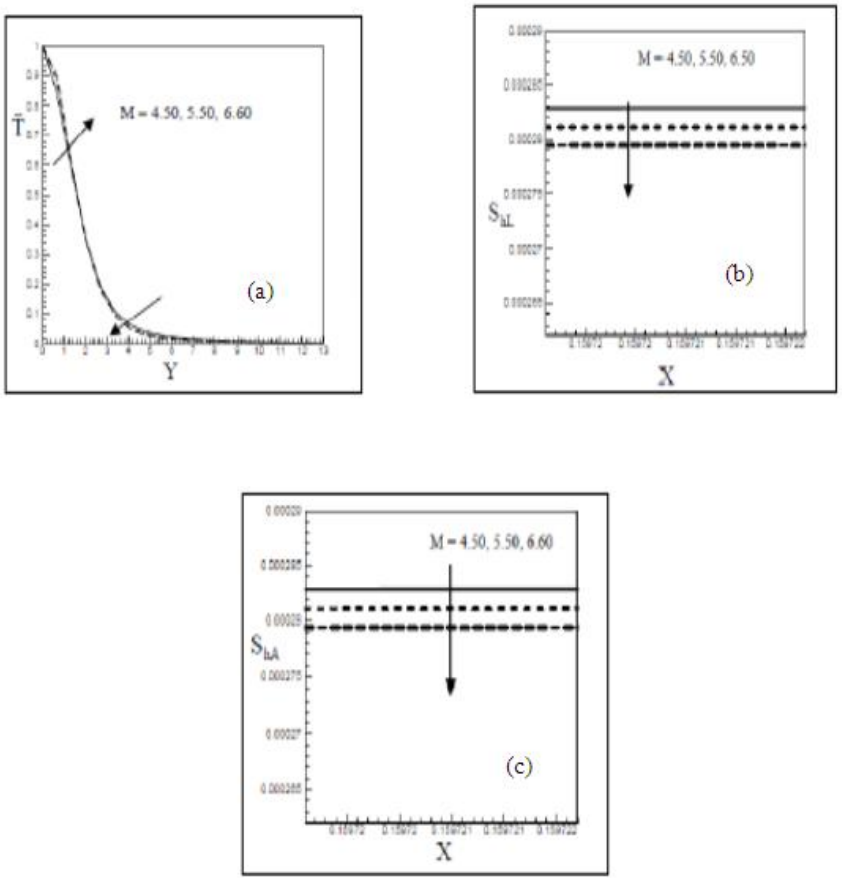

Figure 4 Effect of magnetic parameter (*M*) on (a) temperature profile, (b) local Sherwood number and (c)average Sherwood number taking Gr =2.50,Gm = 2.50, Pr = 7.00, Ec = 0.01, Sc = 0.22, and N = 0.01

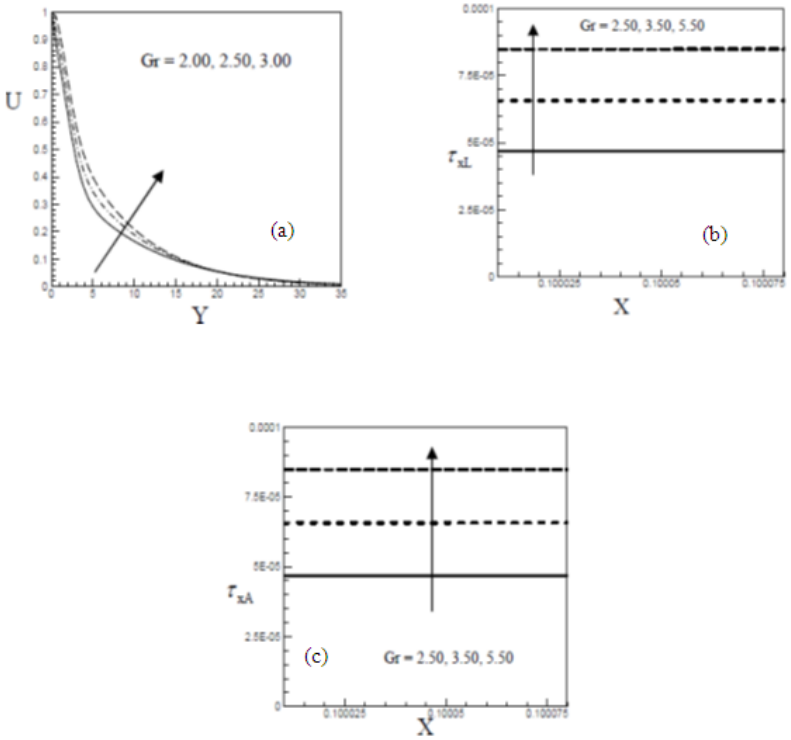

Figure5 Effect of Gr on (a) velocity, (b) local shear stress, (g) average shear stress, (c) average Sherwood number, taking M =4.50,Gm = 2.50, Pr = 7,00, Ec = 0.01, Sc = 0.22, and N = 0.01

It is observed from Fig. 6(a) the temperature profile decreases in the range $0 \le Y \le 3.9$ (approx.) and then increased for the increasing values of Gr . Due to enhancement of Gr the thermal buoyancy effect has tendency to increase, as a result, the rate of heat transfer increase. Thus the temperature profiles increases ($Y > 3.9$). Figures 6(b) and 6(c) elucidate local and average Sherwood numbers for different values of Gr and it is found that both local Sherwood number and average Sherwood number are increasing. Due to increase in the values of Grashof number has the tendency to increase the thermal buoyancy effect. This gives rise to an increase in the induced flow. As a result local Sherwood number and average Sherwood number are increased.

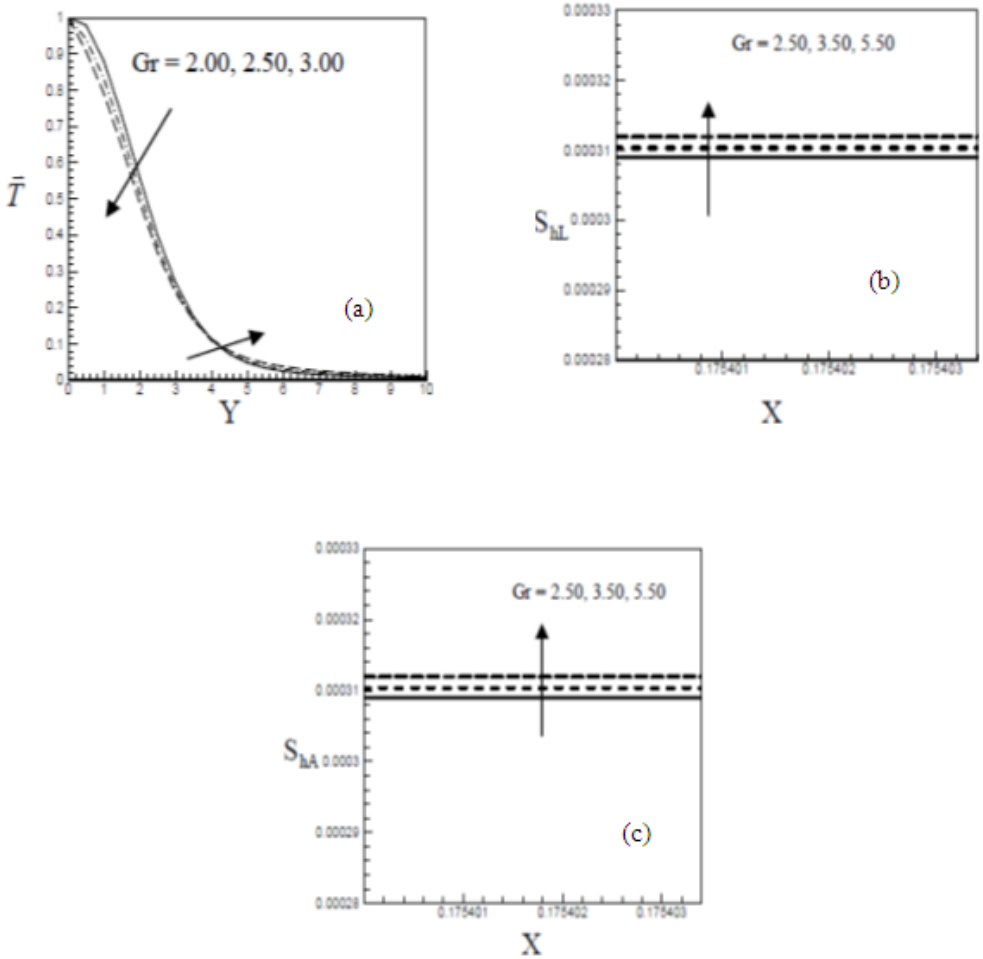

Figure 6 Effect of Gr on (a) temperature, (b) local Sherwood number, and (c) average Sherwood number, taking M =4.50,Gm = 2.50, Pr = 7,00, Ec = 0.01, Sc = 0.22, and N = 0.01.

The concentration profile is decreasing for increasing values of Gr scrutinizes in Fig. 7(a). Figures 7 (b) and 7(c) demonstrate local and average Nusselt numbers which are decreased for increasing values of Gr .

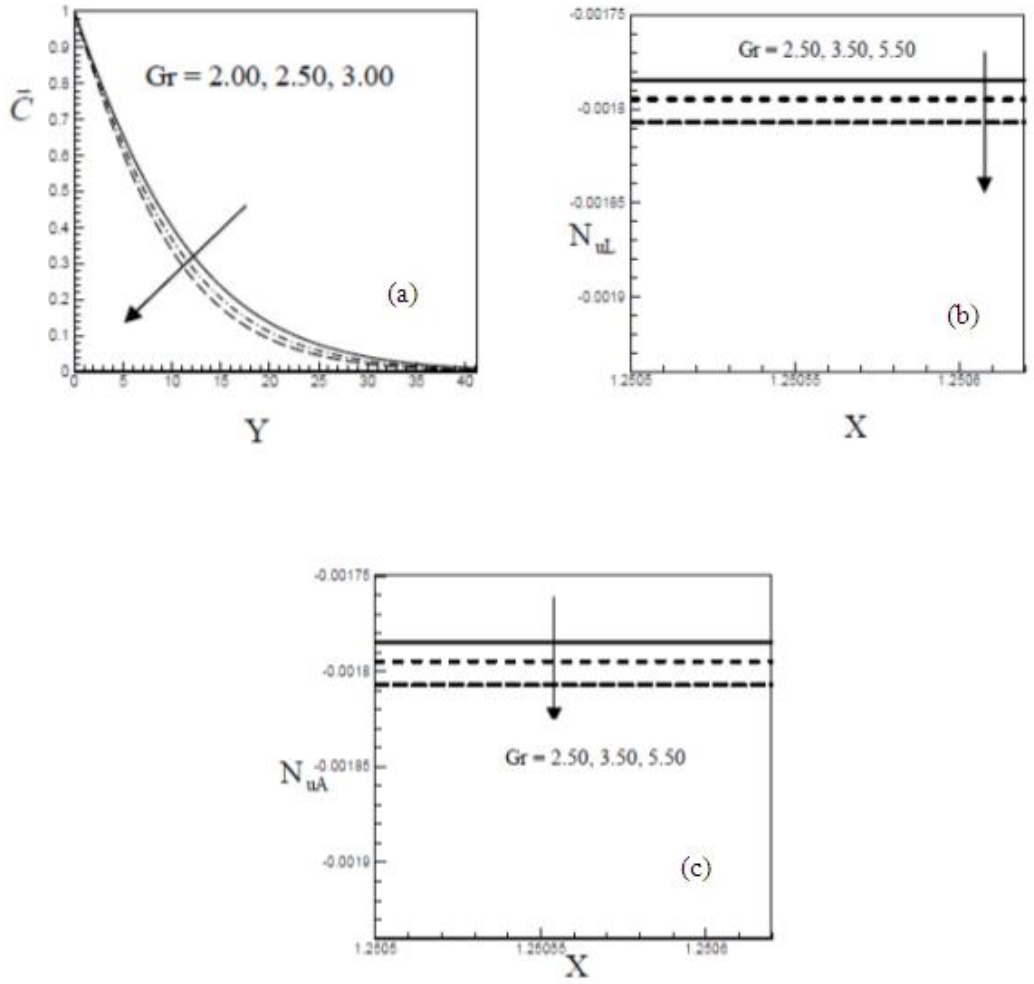

Figure 7 Effect of Gr on (a) concentration profiles, (b) local Nusselt number, and (c) average Nusselt number with M =4.50,Gm = 2.50, Pr = 7,00, Ec = 0.01, Sc = 0.22, and N = 0.01

Figure 8(a) demonstrates the temperature profile for the effect of Pr and found that the temperature profile is increasing in the range $0 \le Y \le 1.9$ and then decreases for increasing values of Pr . It is observed that increase in the Prandtl number, Pr results decrease the thermal boundary layer thickness and in general lower average temperature within the boundary layer. The reason is that smaller values of Pr are equivalent to increase in the thermal conductivity of the fluid and therefore, heat is diffuse away from the heated surface more rapidly for higher values of Pr. Hence in the case of smaller Prandlt number the thermal boundary layer is thicker and the rate of heat transfer is reduced. The local and average Sherwood numbers decrease for increasing values of Pr predict in Figs. (b) and 8(c), respectively.

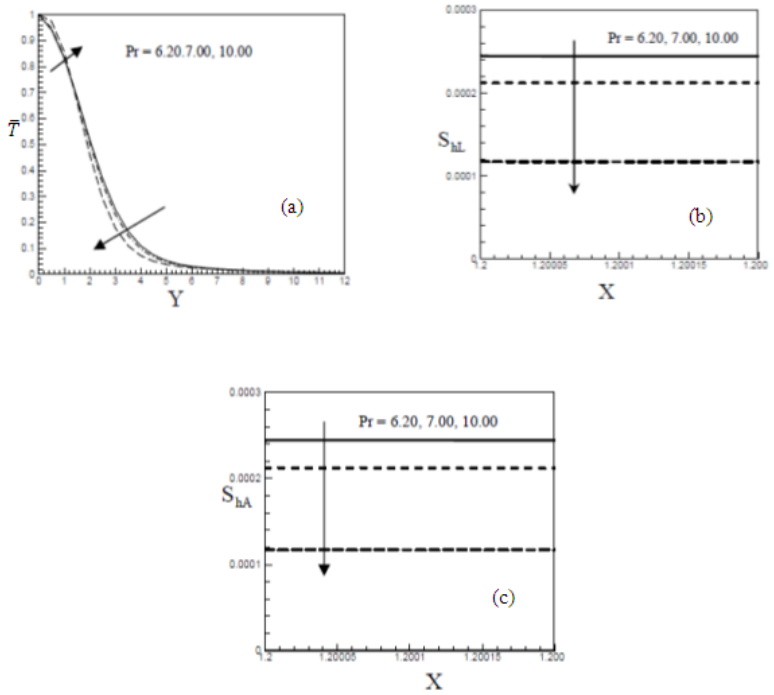

Figure 8 Effect of Pr on (b) temperature, (e) local Sherwood number, (f) local Nusselt number, and average Sherwood number, with M = 4.50, Gr = 2.50, Gm = 2.00, Ec = 0.01, Sc = 0.22, and N = 0.01

Figure 9 (a) demonstrates temperature profile and found that the temperature profile is increasing for increasing values of Ec. In fact the heat energy is stored in liquid due to the frictional heating, thus for the effect of Ec is to enhance the temperature at any point. Figures 9(b) and 9(c) illustrate local and average Sherwood numbers which increased for increasing values of Ec. These are due to the heat energy is stored in liquid due to the frictional heating.

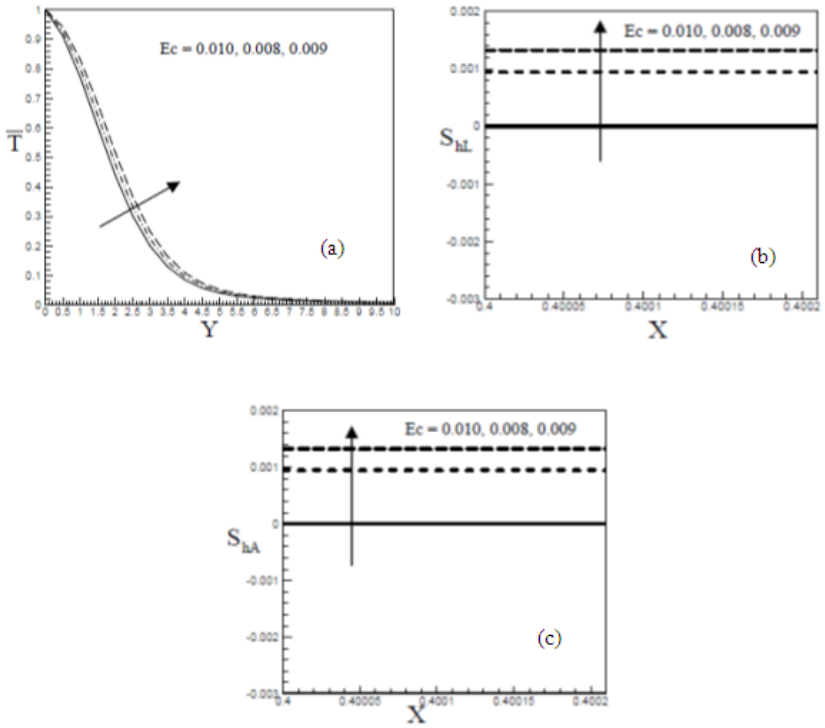

Figure 9 Effect of Ec on (a) temperature profile, (b) local Sherwood number, and (c) average Sherwood number, with M = 4.50,Gr = 2.50, Gm = 2.00, Sc = 0.22, Pr = 6.2, and N = 0.01

Figures 10(a) demonstrates characteristic behavior of concentration profiles for increasing values of Sc taking remaining parameters as constant and found that for the increasing values of Sc the concentration profile decreases depict. The Schmidt number (Sc) quantifies the relative effectiveness of momentum and mass transport by diffusion in the hydrodynamic and concentration boundary layers. As the Schmidt number increases, the concentration profile decreases, this causes the concentration buoyancy effect to decrease complaint a reduction in the fluid velocity. The reductions in the velocity and concentration profile are accompanied by simultaneous reduction in the velocity and concentration boundary layers. It contributes to decrease of concentration of the fluid. Figure 10(b) predicts the local Nusselt number and found that the local Nusselt number is decreasing for increasing values of Sc . The effect of then Sc embodies the ratio of the momentum to the mass diffusivity. It is noticed that as the Sc increases the velocity as well as concentration decreases. This causes the concentration buoyancy effects to decrease yielding a reduction in the fluid velocity. The average Nusselt number decreased for various values of Sc illustrates Fig.10(c).

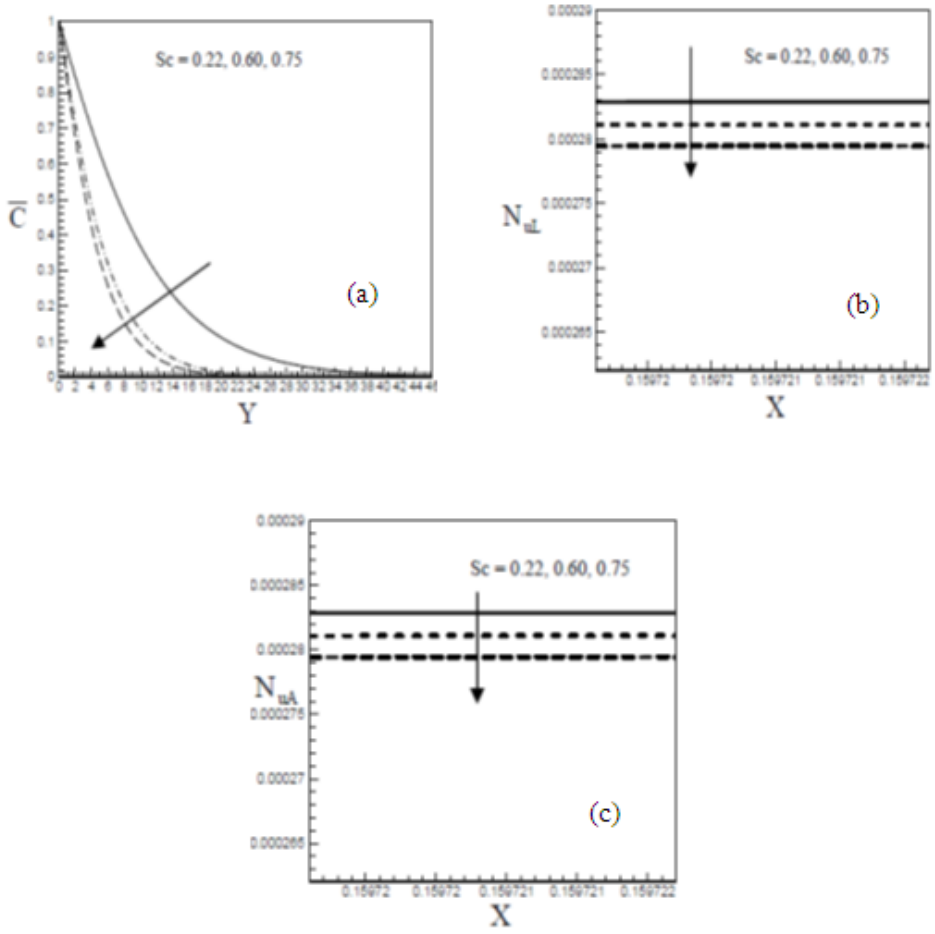

Figure 10 Effect of Sc on (a) concentration profiles, (b) local Nusselt number, and (c) average Nusselt number with M = 4.50,Gr = 2.50, Gm = 2.00, Ec = 0.01, Pr = 6.2, and N = 0.01

Figures 11(a) and 11 (b) depict the velocity and temperature profiles for increasing values of N and observed that both velocity and temperature profiles are decreased. It is fact that, due to increase the values of porosity parameter the tightness of the porous medium increased results in increasing the resistance against the flow, thus the fluid velocity decreases for increasing values of porosity parameter. Figure 11(c) demonstrates concentration profile that is increased for increasing values of N .

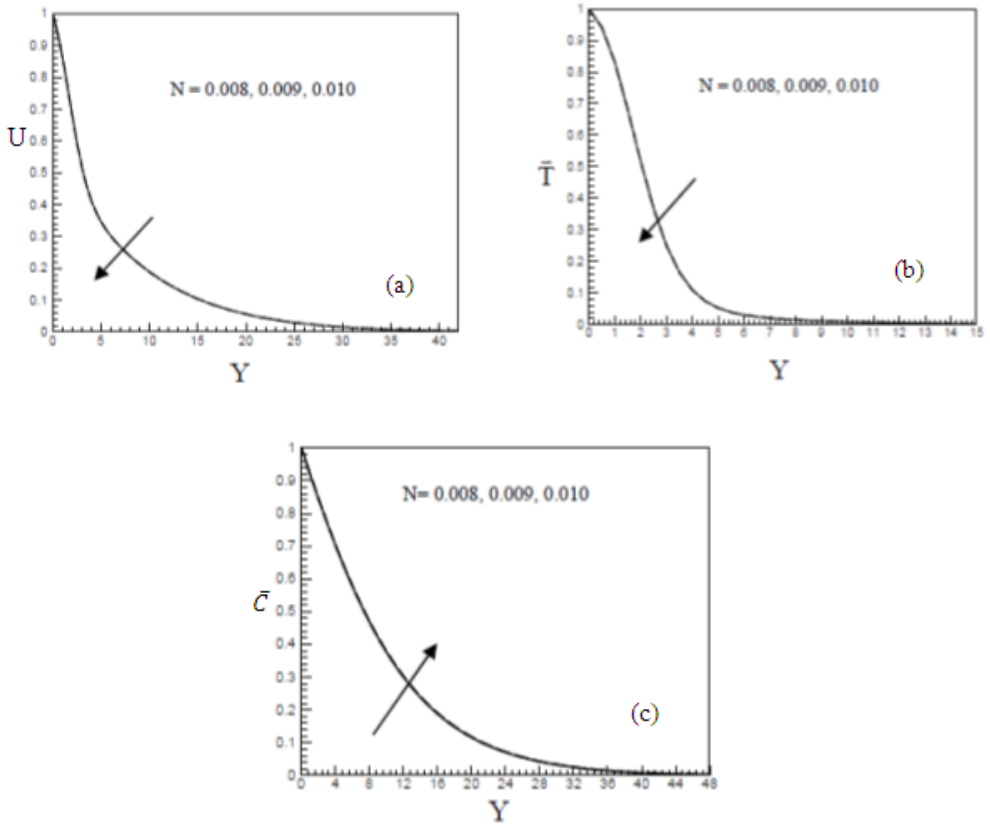

Figure 11 Effect of N on (a) velocity, (b) temperature, and (c) concentration profiles with M = 4.50,Gr = 2.50, Gm = 2.00, Sc = 0.22, Pr = 6.2,andEc = 0.01

VI. Conclusion

In this report the free convection heat and mass transfer has investigated over a vertical plate embedded in porous medium in presence of magnetic field. The effects of concerned parameters on velocity, temperature and concentration profiles as well as local shear stress, Sherwood and Nusselt numbers, average shear stress, Sherwood and Nusselt numbers are investigated and presented graphically. The important results are summarized as follows:

The velocity profile has decreased with increasing of magnetic parameter. On the other hand in a certain interval the temperature profile has increased due to the increasing effect of magnetic parameter and then decreasing. The velocity profile increased for increasing values of Gr which leads to raise the velocity due to the thermal buoyancy force induces pressure gradient. Due to enhancement of Gr the thermal buoyancy effect has tendency to increase, as a result, the rate of heat transfer increase. Thus the temperature profiles increases ($Y > 3.9$).The concentration profile is decreasing for increasing values of Gr . For the effect of Pr the temperature profile is increasing in the range $0 \leq Y \leq 1.9$ and then decreases. Due to the frictional heating the heat energy is stored in liquid for the effect of Ec , consequently enhances the temperature in the boundary layer. For the concentration buoyancy effect to decrease complaint reduction in the fluid velocity due to Schmidt number as a result concentration profile decreases. The porosity parameter has insignificant effect on the velocity, temperature and concentration profiles.

References

[1]. H. Alfvén, Nature **150**, 405 (1942)
[2]. H. Farrokhi., D. O. Otuya, A. Khimchenko and D. Jing, Open access peer-reviewed chapter (2019); DOI: 10.5772/intechopen.87109
[3]. Hierarchically Structured Porous Materials: From Nanoscience to Catalysis, Separation, Optics, Energy, and Life Science - Wiley Online Library (2011) DOI:10.1002/9783527639588. ISBN 9783527639588
[4]. H. A. El-Arabawy, International Journal of Heat and Mass Transfer **46**,1471(2003)
[5]. A. Bejan, K. R. Khair, International Journal of Heat and Mass Transfer **28**, 909 (1985)
[6]. K. D. Singh, , International Journal of Applied Mechanics and Engineering **16**, 277 (2011)
[7]. K. Raghunath, M. Obulesu and R. Sivaprasad, AIP Conference Proceedings **2220**, 130003 (2020)
[8]. R. Choudhury and S. K. Das, Journal of Applied Fluid Mechanics **7**, 603 (2014)

[9]. P. S. Reddy and P. Sreedevi, Multidiscipline Modeling and Structures **17** (2020)
[10]. A. Keya, Mathematical Problems in Engineering **212**, 19 (2012)

M. Jahir, et. al. "MHD Free Convection Heat and Mass Transfer on a Vertical Plate Embedded in Porous Medium." *IOSR Journal of Mechanical and Civil Engineering (IOSR-JMCE)*, 18(2), 2021, pp. 25-37.